[CANCER RESEARCH 62, 2791–2797, May 15, 2002]

Myeloid Leukemias Have Increased Activity of the Nonhomologous End-Joining Pathway and Concomitant DNA Misrepair that Is Dependent on the Ku70/86 Heterodimer

Terry J. Gaymes, Ghulam J. Mufti, and Feyruz V. Rassool[1]

Department of Haematological Medicine, Leukaemic Sciences Laboratories, The Rayne Institute, GKT School of Medicine, Denmark Hill, London SE5 9NU

ABSTRACT

Human myeloid leukemias are characterized by chromosomal abnormalities, including translocations, deletions, and allelic loss. These alterations are known to disrupt the function of genes that contribute to tumor initiation and progression. The mechanism underlying the appearance of these chromosomal alterations is poorly understood. Recent evidence suggests that altered nonhomologous end joining (NHEJ) is associated with the incidence of chromosome abnormalities in mutant rodent cells. This pathway is thought to provide a major mechanism for the repair of double-strand breaks (DSB) in higher eukaryotes. Here, we show that in an *in vitro* assay for DSB end ligation, nuclear extracts prepared from cultured and primary myeloid leukemia cells show a 2–7-fold increase in end-ligation efficiency as compared with mobilized peripheral CD34+ blood progenitor cells (CD34+) and interleukin-2-stimulated peripheral blood lymphocytes from normal healthy donors ($P < 0.001$). Furthermore, using an *in vitro* plasmid *LacZ* gene reactivation assay to determine DSB repair fidelity, nuclear extracts prepared from myeloid leukemia cells showed an increased frequency of misrepair compared with normal control cells ($P < 0.001$). Most importantly, this misrepair in myeloid leukemia cells is associated with large deletions (30–400 bp) within the test plasmids used in our assay. These deletions were not observed using normal hematopoietic cells (<28 bp). Strikingly, we show that the NHEJ proteins, Ku70 and 86, are required for the deletions in myeloid leukemias because preincubating nuclear extracts from leukemic cells with antisera against Ku86 and Ku70 inhibits plasmid reactivation and restores the frequency and size of deletions to control levels. Our findings suggest that an overactive NHEJ system and, specifically, aberrant Ku70/86 activity is a candidate mechanism for chromosomal instability in myeloid leukemias.

INTRODUCTION

Genomic instability is a hallmark of cancers and leukemias. At least two types of genomic instability have been elucidated. These include instability detected in microsatellite repeat DNA sequences and the type of instability resulting in chromosomal deletions, rearrangements, and complete chromosomal loss (aneuploidy; Refs. 1 and 2). Defective repair of mismatched DNA bases, resulting in an increased mutation rate at the nucleotide level and consequent widespread microsatellite instability, can initiate and accelerate the neoplastic process in subtypes of colon, gastric, and endometrial cancers (3). However, the genetic basis for chromosomal instability is poorly understood.

Evidence supports the notion that chromosomal abnormalities can arise through perturbations in the pathways involved in the repair of DSB[2] (reviewed in Refs. 4 and 5). Frequent chromosomal translocations have been demonstrated after induction of DSB (6). Although there are at least two mechanisms for the repair of DSB, NHEJ is regarded as the dominant mechanism for the repair of DBS in mammalian cells (reviewed in Ref. 7). NHEJ has been characterized extensively in rodent cells (reviewed in Ref. 8) and has identified a pathway in which the subunit proteins of the Ku70/Ku86 heterodimer bind free DNA ends at the sites of DSB and are then phosphorylated by DNA-PK activated by the bound Ku70/86 heterodimer (9–11). The targeted free ends are subsequently ligated by DNA ligase IV in conjunction with XRCC4 (12). End-joining reactions can be error prone, containing deletions (<20 bp) back to regions of microhomology of one to six bases (13, 14). Despite the potential role of the NHEJ system in genomic instability in cancer, it has not been extensively studied in primary neoplastic cells.

Leukemias provide an ideal model for the study of mechanisms for chromosomal instability because they demonstrate consistent chromosomal translocations and deletions (15, 16). Thus, we undertook to study the role of NHEJ in myeloid leukemia cell lines and cells from patients with myeloid malignancies. Here, we report a marked overactivity of the NHEJ system in myeloid leukemia cells through which Ku70/86 can induce aberrant ligation of DNA ends, resulting in plasmid deletions in our *in vitro* assays. This system could represent a major pathway through which chromosomal abnormalities may arise in myeloid leukemias.

MATERIALS AND METHODS

Cell Culture. Myeloid cell lines HL60 and K562 were purchased from the American Type Culture Collection. The myelomonocytic cell line, P39, was a kind gift from Richard L. Darley, University of Wales College of Medicine, Cardiff, Wales. These cell lines were cultured at 37°C (5% CO_2) in Dutch modified RPMI 1640 supplemented with 10% FCS, 4 mM glutamine, and 1% penicillin/streptomycin (all purchased from Sigma-Aldrich Co. Ltd., Poole, United Kingdom). MDS92-L was a kind gift from the University of Kyoto, Kyoto, Japan, and cultured as above apart from the addition of 200 units of IL-3 (R&D Systems syprogenitors, Abingdon, United Kingdom).

Mobilized peripheral blood CD34+ progenitor cells (CD34+) were harvested from normal and healthy donors. They were cultured in Iscove's modified Dulbecco's media (Sigma) supplemented with 20% FCS, 4 mM glutamine, and 1% penicillin/streptomycin. Cells were stimulated by adding 10 ng/ml stem cell factor (R&D systems), 10 ng/ml IL-6, and 10 ng/ml IL-3 and grown to a density of 1×10^6/ml for 5 days (17). PBLCs from normal subjects were prepared from heparinized blood using Hypaque-Ficoll (Sigma) gradients and cultured at 1×10^6/ml in RPMI 1640, supplemented with 10% FCS, 4 mM glutamine, and 1% penicillin/streptomycin. PBLCs were stimulated by adding phytohemattagluttinin (Sigma) for 48 h, washed several times to remove phytohemattagluttinin, and then cultured in 1 unit/ml IL-2 for a maximum of 14 days. Newly diagnosed and untreated myeloid leukemia patient samples were received from hematology clinics. Clinical diagnosis and cytogenetics analysis was made on each sample before primary cell harvesting using Hypaque-Ficoll gradients. The mononuclear fraction was isolated from 10–20 ml of CML or AML peripheral blood. Cytospins of these fractions were examined morphologically after May-Grunwald Giemsa staining and revealed the presence of >95% of the CML cells or AML blasts, respectively; lymphocyte and monocyte contamination was negligible. Primary cells were cultured at 1×10^6/ml in RPMI 1640, supplemented with 10% FCS, 4 mM

Received 9/17/01; accepted 3/7/02.

The costs of publication of this article were defrayed in part by the payment of page charges. This article must therefore be hereby marked *advertisement* in accordance with 18 U.S.C. Section 1734 solely to indicate this fact.

[1] To whom requests for reprints should be addressed, at Department of Haematological Medicine, Leukaemic Sciences Laboratories, The Rayne Institute, GKT, Denmark Hill, London SE5 9NU. Phone: 44-207-848 5821; Fax: 44-207-848 5814; E-mail: feyruz.rassool@kcl.ac.uk.

[2] The abbreviations used are: DSB, double-strand break; NHEJ, nonhomologous end-joining; DNA-PK, DNA-protein kinase; IL, interleukin; PBLC, peripheral blood lymphocyte; AML, acute myelogenous leukemia; CML, chronic myelogenous leukemia; v/v, volume for volume; PMSF, phenylmethylsulfonyl fluoride; KOAc, potassium acetate.

glutamine, and 1% penicillin/streptomycin for 24 h before nuclear extraction. Typically, between $2 \times 10^6 - 10^7$ cells were used for the preparation of nuclear extracts.

Preparation of Nuclear Extracts. Nuclear extracts were prepared based on the protocol devised by Jessberger and Berg (18). Log phase cells (2×10^6/ml) were centrifuged in a swing-out rotor at $150 \times g$ for 10 min at 4°C. The pellet was resuspended in ice-cold nuclei isolation buffer [3.75 mM Tris-HCl (pH 7.5), 0.05 mM spermine, 0.125 mM spermidine, 0.5 mM EDTA, 20 mM KCl, 0.1 mM PMSF, 0.1% (v/v) aprotinin, and 0.5% (v/v) thiodiglycol; Sigma] at 2×10^6cells/ml buffer and centrifuged as before. The cells were resuspended in ice-cold nuclei isolation buffer, and this procedure was repeated once more. The cells were resuspended in ice-cold nuclei isolation buffer II [3.75 mM Tris-HCl (pH 7.5), 0.05 mM spermine, 0.125 mM spermidine, 0.5 mM EDTA, 20 mM KCl, 0.1 mM PMSF, 0.1% (v/v) aprotinin, 0.5% (v/v) thiodiglycol, and 0.1% (w/v) digitonin] at 3.75×10^6cells/ml buffer, dounce homogenized using a Wheaton B pestle, layered on 0.25 M sucrose gradients, and centrifuged at $150 \times g$ for 10 min at 4°C. Nuclei pellets were resuspended in ice-cold isolation buffer II and pooled. Nuclei were lysed by suspending in ice-cold nuclei lysis buffer [10 mM HEPES (pH 7.5), 350 mM KCl, 0.2 mM EDTA, 3 mM $MgCl_2$, 0.001 mM DTT, 0.2 mM PMSF, 0.2% aprotinin (v/v), and 15% (v/v) glycerol; Sigma] and incubated on ice for 30 min. The nuclei were then centrifuged at $70,000 \times g$ for 60 min at 4°C. The supernatant was retained and dialyzed for 3 h against E buffer [20 mM Tris-HCl (pH 8.0), 0.1 mM KOAc, 20% (v/v) glycerol, 0.5 mM EDTA, and 1 mM DTT; Sigma], fast frozen, and stored at −80°C.

Plasmids and Antibodies. Puc18 was linearized with *Eco*RI (MBI Fermentes, Cleveland, United Kingdom), dephosphorylated with calf intestine alkaline phosphatase (Promega, Southampton, United Kingdom), and ^{32}P-labeled with T4 polynucleotide kinase (Promega). Goat polyclonal antisera raised against Ku86, Ku70, DNA-PKcs, and Oct-2, and their respective blocking peptides were purchased from Santa Cruz Biotechnology (Santa Cruz, CA). Ku86 and Ku70 blocking peptides mapped to the COOH terminus (amino acids 713–730 and 590–608) of their respective proteins. DNA-PKcs blocking peptide mapped to the NH_2 terminus (amino acids 2–21). Rabbit polyclonal antisera raised against Rad51 was a kind gift from Stephen West, Imperial Cancer Research Fund (South Mimms, United Kingdom).

End Ligation Assay. Assays were performed according to the protocol of Baumann and West (19). Reactions (10 μl) were performed in 50 mM triethanolamine-HCl (pH 7.5), 60 mM KOAc, 50 μM deoxynucleotide triphosphates, 2 mM ATP, 1 mM DTT, and 100 μg/ml BSA. Nuclear cell extract (containing 3 μg of protein; Ref. 20) was incubated for 5 min at 37°C before the addition of ^{32}P-labeled pUC18 (10 ng). A DSB was introduced previously into this plasmid by digestion with *Eco*RI restriction enzyme, thus creating a 5′ protruding single strand. These specific DSBs were shown by Baumann and West (19) to be a substrate for end ligation. The end-ligation mixture was incubated for 24 h at 18°C. ^{32}P-labeled products were deproteinized by passing the mixture through filter spin columns (Qiagen, Crawley, United Kingdom) and analyzed by electrophoresis on 0.6% agarose gels. End-ligation efficiency was quantitated by phosphorimaging and two-dimensional densitometry analysis (Automatic Image Data Analyzer). End-ligation efficiency was assessed by dividing the densitometry readings for the sum of all converted plasmid products by the sum of all products. Using these measurements, we were able to compare the DSB ligation efficiencies between different cell samples. Nuclease activity was reduced to negligible levels when nuclear, rather than cell, extracts were prepared. Nuclease activity was examined in our samples by incubating nuclear extracts from different sources, with linearized and labeled plasmid DNA without end-ligation buffer for 24 h at 18°C. The plasmid DNA was then purified using filter columns and then incubated with 20 units of T4 DNA ligase in T4 DNA ligase buffer (MBI Fermentes) for 24 h at 12°C. The DNA was purified again, and then the products were run on 0.6% agarose gels. Overall, nuclease activity was obtained by simply dividing the phosphor image signal for nuclear extract end-ligation assays by the signal obtained from assays lacking nuclear extract.

Plasmid Reactivation Assay. Nuclear extracts were prepared as for the end-ligation assay. We used the DNA repair fidelity assay devised by North *et al.* (21). For the assay, 2 μg of *Eco*RI linearized pUC18 were incubated with 3 μg of nuclear extract. Reactions (10 μl) were carried out in 50 mM triethanolamine-HCl (pH 7.5), 60 mM KOAc, 50 μM deoxynucleotide triphosphates, 2 mM ATP, 1 mM DTT, and 100 μg/ml BSA. The mixture was incubated for 24 h at 18°C. Plasmid DNA was purified from extract by passing it down a filter column and then diluted 3-fold in 10 mM Tris (pH 8)-1 mM EDTA buffer, and 10 ng were used to transfect *Escherichia coli* strain DH5α. Transformed cells were plated out on Luria-Bertani agar plates, including 100 μg/ml ampicillin, 20 mg/ml X-gal, and 200 mg/ml isopropyl-1-thio-β-D-galactopyranoside. To allow for spontaneous rejoining/incomplete *Eco*RI cutting, assay controls were conducted without nuclear extract. The number of colonies generated was subtracted from extract-treated plasmid colonies. In addition, to correct for bacterial plating numbers and determine whether nuclease activity was affecting plasmid efficacy, cells were plated on Luria-Bertani agar without ampicillin. Primers around the *Eco*RI site were designed to give a PCR product of 628 bp corresponding to nucleotides 150–777 bp. Colony PCR was performed on blue and white colonies to determine the size of the deletion. Sequencing of PCR products was performed on an ABI prism 377 DNA sequencer using Thermo Sequenase II dye terminator cycle sequencing premix kit (Perkin-Elmer, Warrington, United Kingdom) in accordance with the manufacturer's instructions.

Antibody Abrogation Studies. For antibody abrogation studies, dilutions of antisera (100 μg/ml) were incubated in the reaction mixture. Antibodies were blocked with 5-fold excess (by weight) of blocking peptide in a small volume of PBS. The blocking reaction was incubated overnight at 4°C.

RESULTS

Ligation Efficiency Assays

Myeloid Leukemia Cell Lines. Using the ligation efficiency assay ("Materials and Methods"), we compared the ligation efficiency in nuclear extracts from several established myeloid leukemia cell lines [HL60 (promyelocytic leukemia), K562 (CML → erythroleukemia), P39 and MDS92-L (myelodysplastic syndrome → myeloblastic)] with CD34+ ($n = 5$) and PBLCs ($n = 4$) from different normal and healthy individuals as controls. Cytogenetic analysis by standard G-banding techniques confirmed that cell lines HL60, K562, P39, and MDS92-L showed multiple chromosome abnormalities identified previously (Table 1; Refs. 22 and 23). All experiments were performed with 3 μg of nuclear extract protein at 18°C for 24 h, within the linear range of the end-ligation reaction, *i.e.*, conditions whereby all monomer plasmids were not converted to ligation products (data not shown). No significant nuclease activity was observed in our samples, which could potentially affect end-ligation results; Fig. 1*A* shows that T4 DNA ligase can ligate with equal efficiency both plasmid DNA incubated without nuclear extracts (*Lane 1*), and plasmid DNA incubated with nuclear extracts from myeloid leukemias. Data from three

Table 1 *Disease and cytogenetic characteristics of myeloid cell lines and primary cells tested for NHEJ*

Myeloid leukemic cell	Chromosome abnormalities	Mean end-ligation efficiency %
Cell lines		
HL60	−5, −8, −17, + unidentified chr.	56
K562	Ph+ t(9;22), t(15;18), −3p, −9p	33
P39	6q+, 9q+, t(14;16)	46
MDS92-L	−5q [del.5q13q35], −7, −12, −13	48
Primary cells		
CML patient 1	Ph+ t(9;22)	46
CML patient 2	Ph+ t(9;22)	49
CML patient 3	Ph+ t(9;22)	52
CML patient 4	Ph+ t(9;22)	56
CML patient 5	Ph+ t(9;22)	51
CML patient 6	Ph+ t(9;22)	43
CML patient 7	Ph+ t(9;22)	37
CML patient 8	Ph+ t(9;22)	47
CML patient 9	Ph+ t(9;22)	29
AML patient 1 (FAB M4)	No abnormalities	36
AML patient 2 (M4)	inv(16)	43
AML patient 3 (M2)	t(1;12)	50
AML patient 4 (M4)	Del. 5q13-31, −7, −17, −20	59
AML patient 5 (M5)	t(1;12)	43
AML patient 6 (M1)	No abnormalities	64

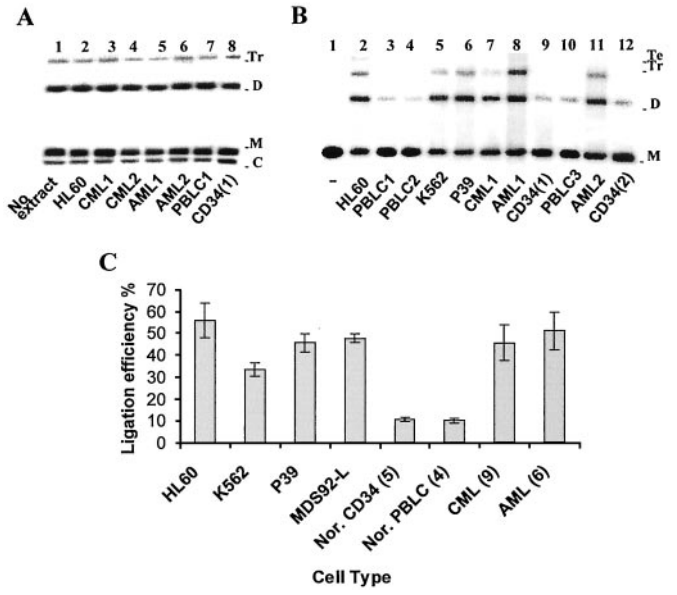

Fig. 1. Ligation efficiency is increased in myeloid leukemia cells. *A*, evaluation of nuclease activity in different nuclear extracts from myeloid leukemia cells. Agarose gel of ligated pUC18 after incubation with T4 DNA ligase following preincubation with nuclear extracts. *Lane 1*, T4 DNA ligase without nuclear extract; *Lane 2*, HL60 cell line; *Lanes 3–4*, CML samples ($n = 2$); *Lanes 5–6*, AML samples ($n = 2$); *Lane 7*, normal PBLCs; *Lane 8*, normal CD34+. A portion (3 μg) of nuclear extract per sample was used (*C*, closed covalent circle; *M*, monomer; *D*, dimer; *Tr*, trimer). *B*, agarose gel of ligated pUC18 after incubation with nuclear extracts. *Lane 1*, no nuclear extract; *Lane 2*, HL60; *Lanes 3*, *4*, and *10*, normal PBLCs; *Lane 5*, K562; *Lane 6*, P39; *Lane 7*, CML sample; *Lanes 8* and *11*, AML samples; *Lanes 9* and *12*, normal CD34. A portion (3 μg) of nuclear extract per sample was used (*M*, monomer; *D*, dimer; *Tr*, trimer; *Te*, tetramer). *C*, bar graph of ligation efficiencies in myeloid leukemia cells compared with normal CD34+ and normal PBLCs. Ligation efficiency was calculated by two-dimensional densitometry measurement of bands for converted plasmid divided by total band intensities. The mean ligation efficiencies for four myeloid leukemia cell lines (HL60, K562, P39, and MDS92-L), nine CML patients, and six AML patients as compared with normal CD34+ [mean ($n = 5$)] and normal PBLCs [mean ($n = 4$)]. A portion (3 μg) of nuclear extract per sample was used to determine end-ligation efficiency.

to five assays with each cell line were consistent and show that the mean ligation efficiency was increased significantly (Fig. 1, *B* and *C*) in the leukemic cells (33.5–55.8%) as compared with normal CD34+ [9.4–11.6%; mean 45.6 *versus* 10.5% ($n = 5$), $P < 0.001$] and normal PBLCs [8.2–11.6%; mean 45.6 *versus* 9.9% ($n = 4$), $P < 0.001$; data for each cell line shown in Table 1]. In addition, a range of normal cells, including WI38 fibroblasts, show end-joining efficiencies similar to the above normal cells (data not shown).

Primary Myeloid Leukemia Cells. To assess ligation efficiency for primary myeloid leukemia cells, nuclear extracts were prepared from the mononuclear cell fractions of nine newly diagnosed and untreated CML and six newly diagnosed and untreated AML patients. Cytogenetic analysis for each patient sample was performed by standard G-banding techniques (Table 1). Ligation efficiencies of myeloid leukemias were compared with the CD34+ [10.5% ($n = 5$)] and PBLCs [9.9% ($n = 4$)] from healthy individuals as detailed above. For the different myeloid diseases, the range of ligation efficiencies were as follows: CML, 29–56% (mean 46%) and AML, 43.7–64% (mean 51%). These results demonstrate that the ligation efficiency is markedly increased in primary myeloid leukemic cells as compared with normal CD34+ and normal PBLCs ($P < 0.001$; Fig. 1*C* data for each patient sample shown in Table 1).

To confirm that proteins involved in NHEJ are responsible for increased ligation efficiencies of DSBs in leukemic cells, nuclear extracts from the HL60 cell line (Fig. 2, *A* and *B*), an AML patient (Fig. 2, *C* and *D*), and normal CD34+ progenitor cells (Fig. 2, *E* and *F*) were incubated with increasing concentrations of antibodies to Ku86, Ku70, and DNA-PKcs. The results of three experiments were consistent, and Fig. 2 illustrates that plasmid ligation was inhibited with increasing concentrations of antibodies specific for all proteins. Control antibodies for proteins, such as Rad51 (Fig. 2, *B*, *D*, and *F*), Oct 2, and antibodies to Ku86, Ku70, and DNA-PKcs, prebound to their cognate peptides showed no decrease in end-joining efficiency with increasing antibody concentration. End joining in our assays thus was the result of Ku-dependent repair, as incubation of anti-Ku86 (1:10), anti-Ku70 (1:10) and anti-DNA-PKcs (1:10) completely abrogated ligation activity in all samples tested (Fig. 2*G*). These results

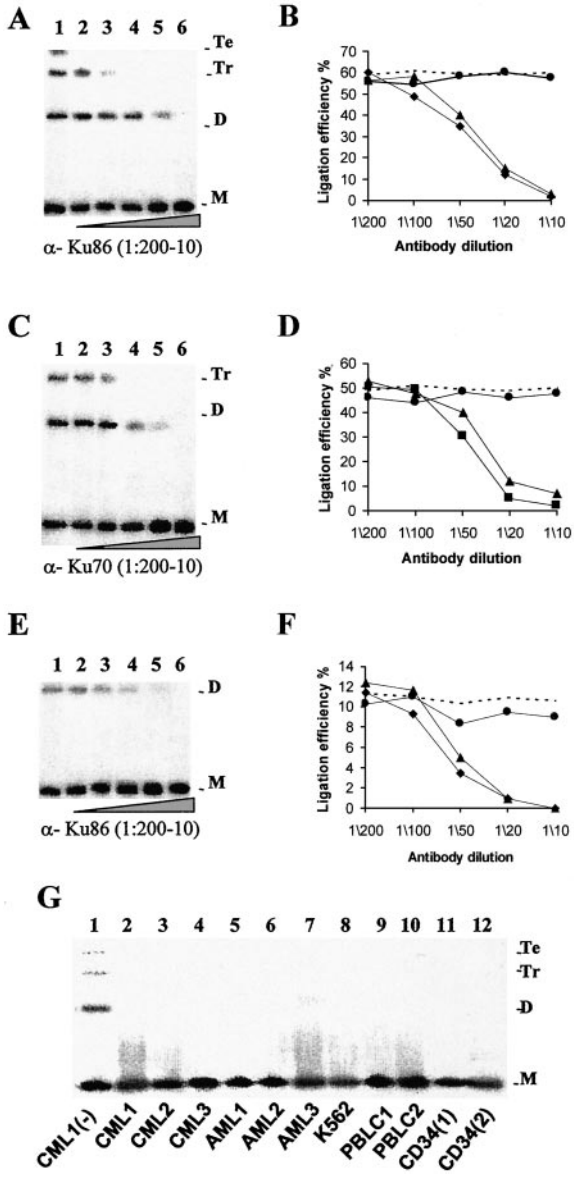

Fig. 2. Ligation efficiency is abrogated with increasing concentration of antibodies against NHEJ proteins. Agarose gels of ligated pUC18 after incubation with nuclear extracts containing antibodies (1:200–1:10; *Lanes 2–6*) to Ku86 or Ku70. Results for the HL60 cell line (*A*), an AML sample (*C*), and a normal CD34+ sample (*E*). A portion (3 μg) of nuclear extract per sample was used (*M*, monomer; *D*, dimer; *T*, trimer; *Te*, tetramer). *B*, *D*, and *F*, ligation efficiency with increasing concentration of antibodies to NHEJ proteins incubated with nuclear extracts from HL60 cells (*B*), AML cells (*D*), and normal CD34+ cells (*F*). Anti-Ku86 (◆), anti-DNA-PKcs (▲), anti-Ku86 + blocking peptide (····), anti-Ku70 (■) and anti-Rad51 control (●). *G*, agarose gel of ligated pUC18 after incubation of nuclear extracts containing a 1:10 dilution of anti-Ku86 antibody. *Lane 1*, pUC18 ligation in a CML sample with no anti-Ku86 added; *Lanes 2–4*, CML samples ($n = 3$); *Lanes 5–7*, AML samples ($n = 3$); *Lane 8*, K562; *Lanes 9–10*, normal PBLC samples ($n = 2$); *Lanes 11–12*, normal CD34+ samples ($n = 2$). A portion (3 μg) of nuclear extract per sample was used.

Table 2 *Number of bacterial colonies counted in misrepair assays*

Cell type	No. of experiments	No. of plates used	No. of colonies per plate[a]	Mean no. of background colonies per plate
HL60, K562	5	10	110–141	6
AML (6)	5	10	125–153	9
CML (9)	5	10	119–146	8
PBLC (4)	5	16	64–85	6
CD34+ (4)	5	16	59–81	6
HL60 + Ku86 (all diln.)	5/diln.	10–20/diln	65–148	9
HL60 + Ku70 (all diln.)	5	10–20/diln	60–139	10
HL60 + DNA-PKcs	5	10–20/diln	59–162	9
AML + Ku86 (all diln.)	5/diln.	10–20/diln	48–139	8
AML + Ku70 (all diln.)	5	10–20/diln	59–129	7
AML + DNA-pKcs	5	10–20/diln	61–140	6
CD34 + Ku86 (all diln.)	5/diln.	10–20/diln	58–60	4
CD34 + Ku70 (all diln.)	5	10–20/diln	59–58	2
CD34 + DNA–PKcs	5	10–20/diln	51–60	6

[a] Number of colonies after subtraction of background colonies.

confirm previous results by Baumann and West (19) that the assay measures NHEJ; it is dependent on Ku86, Ku70, and DNA-PK; and shows that this pathway is responsible for the increased DSB ligation efficiency observed in myeloid leukemia cells.

Repair Fidelity Assays

NHEJ is an error-prone mechanism that often results in the excision and deletion of several bases (13, 14). Therefore, we determined whether the increased NHEJ in leukemic cells was associated with an increased frequency of DNA deletions at the site of repair. We used the DNA repair fidelity assay devised by North *et al.* (21). This plasmid reactivation system determines the ability of nuclear extracts to correctly rejoin a single *Eco*RI-cut DSB (5′ protruding single strand) within the *lacZα* gene of the pUC18. Correct ligation of the DSB without the loss or addition of bases resulted in blue colonies, whereas faulty repair would result in white colonies. The percentage of white colonies over total colonies gave the frequency of misrepair after correction for spontaneous plasmid rejoining and bacterial cell viability controls. Table 2 shows the number of colonies examined after subtraction of the low frequency of background colonies observed. As Fig. 3*A* illustrates, the mean frequency of misrepair from five different sets of experiments was increased in both HL60 (6.1%), K562 (5.7%), and patient samples [CML, 4.5–7% (mean 5.8%) and AML, 5.6–8% (mean 7%)], compared with normal CD34+ [1.6–2.2% (mean 1.81%)] and PBLCs [1.8–2.5% (mean 2.1%); $P < 0.001$].

Colony PCR was performed on blue and white colonies from each of the above experiments using primers located on either side of the DSB. Blue colonies (*b*) should yield a normal PCR product of 628 bp, indicating proper repair of the damaged plasmid. PCR of 12–20 white (*w*) colonies/experiment derived from incubations of linearized pUC18 with normal CD34+ and normal PBLC cell nuclear extracts yielded PCR products with small deletions of <28 bp (Fig. 3, *B–D*). However, PCR analysis of 12–20 white colonies/experiment derived from assays with myeloid leukemia cell extracts showed a dramatic increase in the number of large deletions (29–400 bp; Fig. 3, *C* and *D*). Sequencing of 6 randomly picked white colonies derived from experiments using HL60 nuclear extracts confirmed that in all 6 clones, deletions encompassed the original *Eco*RI DSB, and the deleted region ranged from 81 to 387 bp (Fig. 4). Analysis of DNA sequences at the ligation site correspond to regions of microhomology found on either side of the breakpoint junctions in the wild-type plasmid (Fig. 4).

To determine whether the inappropriate activity of one of the proteins of the NHEJ pathway is responsible for aberrant DSB rejoining observed in myeloid leukemic nuclear extracts, repair fidelity assays were repeated with nuclear extracts from the HL60 cell line, one AML patient, and normal CD34+ progenitor cells in the presence of increasing concentrations of antibodies against Ku70, Ku86, or DNA-PKcs. Results from five different experiments with each antibody at different concentrations were consistent and indicate a general decrease in total colonies observed with all three antibodies (Fig. 5*A*), in accordance with the antibody abrogation of end joining shown previously in our ligation assays (Fig. 2, *D–F*). In the plasmid reactivation assay, incubation with antisera to Ku70, Ku86, or DNA-*PKcs* at concentrations that were still permissive for DSB repair (2–20-fold higher dilution than used above) allowed calculation of DNA misrepair frequencies. The number of colonies counted per experiment is indicated in Table 2. Experiments were repeated three to five times with consistent results. We showed that at an antibody dilution of 1:20 anti-Ku86-treated extracts restored the frequency of misrepair to normal levels in both HL60 and AML cells [6.4 (mean) to 3 (mean); $P < 0.001$ ($n = 6$); Fig. 5*B*]. Anti-Ku70-treated extracts (1:20) also restored the frequency of misrepair to normal levels [6.4 (mean) to 2.4 (mean); $P < 0.001$ ($n = 6$)] in both the HL60 and AML cells (Fig. 5*C*). However, using an antibody to DNA-PKcs, there was no change in the mean frequency of misrepair (Fig. 5*D*). In addition, incubation of a CML extract with increasing concentrations of Ku86 or Ku70 showed similar restoration of frequency of misrepair (data not shown).

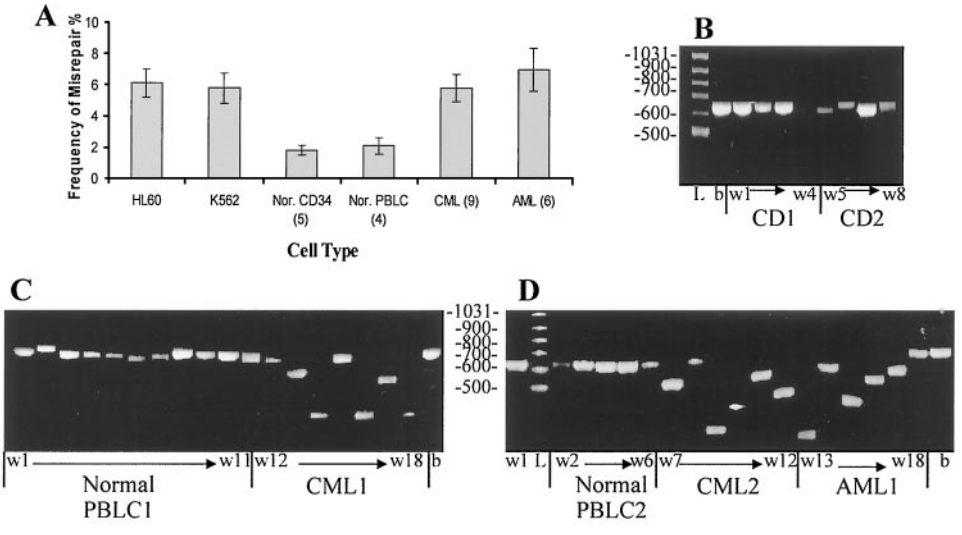

Fig. 3. The infidelity of repair is dramatically increased in myeloid leukemia cells as compared with CD34+ progenitor cells and normal PBLCs. *A*, misrepair frequencies in myeloid leukemia cell lines (*HL60* and *K562*), CML samples ($n = 9$), AML samples ($n = 6$), normal CD34+ ($n = 5$), and normal PBLCs ($n = 4$). The frequency of misrepair was calculated by counting the number of white colonies as a percentage of the total colonies derived from a LacZα reactivation assay (26). In *B–D*, colony PCR was performed on blue (*b*) and white (*w*) colonies using primers located on either side of the DSB. Blue colonies, which have an intact *LacZα* gene, yield a normal PCR product of 628 bp. PCR of misrepaired colonies derived from plasmid reactivation assays in nuclear extracts from normal CD34+ (*B*; *CD1*, donor 1, *w1-w4*; *CD2*, donor 2, *w5-w8*). *L*, DNA ladder (bp) and normal PBLC1 (*C*; donor 1, *w1–11*), one CML sample (*w12–18*), and blue colony (*b*) and normal PBLC2 (*D*; donor 2, *w1–6*), CML2 sample (*w7–12*), and one AML patient (*w13–18*).

A

Bacterial clone	PCR product size (bp)	Size of deletion (bp)	Deleted region (nt)	DNA repeat sequence at DSB
Blue	628	-	-	-
w1	391	237	221-459	CGTAA
w2	371	257	450-708	CTCG
w3	169	459	283-748	GGCGA
w4	441	187	351-539	GTAA
w5	501	127	325-453	GCTG
w6	570	58	405-464	AGCT

B

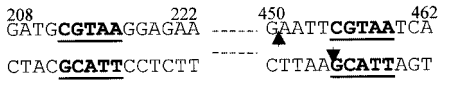

C

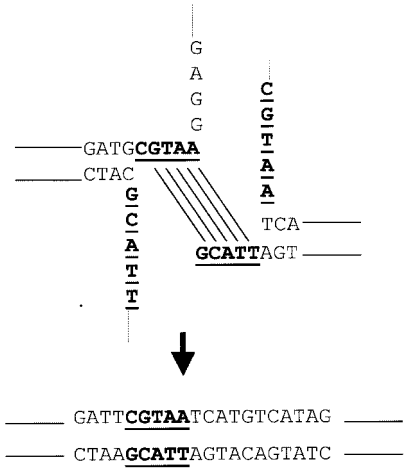

Fig. 4. End-ligation occurs through alignment of microhomologies: sequence analysis of misrepaired plasmids. DNA sequencing of PCR products of six white colonies from misrepair assays using HL60 nuclear extracts show large deletions around the *Eco*RI restriction site. Short tracks of nucleotide microhomology were found around the breakpoint junctions (forward strand of microhomology shown; *A*). DNA sequences from normal pUC18 showing the *Eco*RI restriction site (*arrows*) and microhomologous sequences on either side of the putative breakpoint junction for clone HL60-w1 (repeat sequences in bold and underlined; *B*). Putative ligation of DNA ends using microhomologous sequences, resulting in a large (237 bp) deletion (*C*).

Experiments using extracts from normal CD34+ cells showed no change in the frequency of misrepair with increasing concentration of antibody. Controls using blocking peptides specific for anti-Ku70 and anti-Ku86 in our assays showed no decrease in either total colony numbers or the mean frequency of misrepair with increasing antibody concentration (Fig. 5, *B–D*).

PCR analysis of a total of 20–50 white colonies from each antibody dilution from three anti-Ku86-treated experiments revealed there was a dramatic reduction in the size of deletions compared with extract only controls (Fig. 6). In HL60, the frequency of aberrant deletions was reduced from 75 (mean) to 5% [mean ($n = 3$); $P < 0.001$]. In extracts from an AML patient, the frequency of aberrant deletions was reduced from 70 (mean) to 10% [mean ($n = 3$); $P < 0.001$; Fig. 6*E*]. PCR analysis of a total of 20–50 white colonies from each antibody dilution from experiments using anti-Ku70 showed a similar reduction in the size of deletions. In HL60, the frequency of aberrant deletions was reduced from 70 (mean) to 8% [mean ($n = 3$); $P < 0.001$]. In extracts from an AML patient, the frequency of aberrant deletions was reduced from 70 (mean) to 6% [mean ($n = 3$); $P < 0.001$; Fig. 6*F*]. In addition, PCR analysis of 20–50 white colonies from each antibody dilution from three anti-DNA-PKcs-treated experiments showed no change in sizes of deletions detected (Fig. 6*G*). Thus, titration studies with antibodies to key NHEJ repair proteins strongly indicate that Ku70 and Ku86 are required for the infidelity of accompanying DSB repair.

To determine whether increased expression of NHEJ proteins could account for the significant increase in end-joining activity and concomitant infidelity, Western blot analysis of NHEJ proteins (Ku70, Ku86, DNA-Pkcs, Mre11, DNA ligaseIV, XRCC4, and Rad51; a DSB repair protein not involved in NHEJ) was performed of cell lysates from six AML, four CML, myeloid cell lines (HL60, P39, K562, and MDS-92L), and controls (CD34+, $n = 2$; PBLCs, $n = 2$). No significant differences in steady-state expression of NHEJ proteins compared with controls were observed (data not shown).

DISCUSSION

The NHEJ pathway has been explored extensively in rodent cells, human cells with engineered mutations in component proteins, or cells containing engineered mutations. Here, we show for the first time that in a native human acute and chronic myeloid leukemia setting, the overall NHEJ activity is constitutively increased, compared with normal hematopoietic cells. Furthermore, NHEJ over-activity shows a striking impairment of DSB repair that is manifested by DNA deletions of ≤400 bp within test plasmids in our *in vitro* assays and suggests an important mechanism through which chromosome instability may arise in human myeloid leukemias.

Titration studies with antibodies to key NHEJ repair proteins strongly indicate that Ku70 and Ku86 are responsible for the infidelity

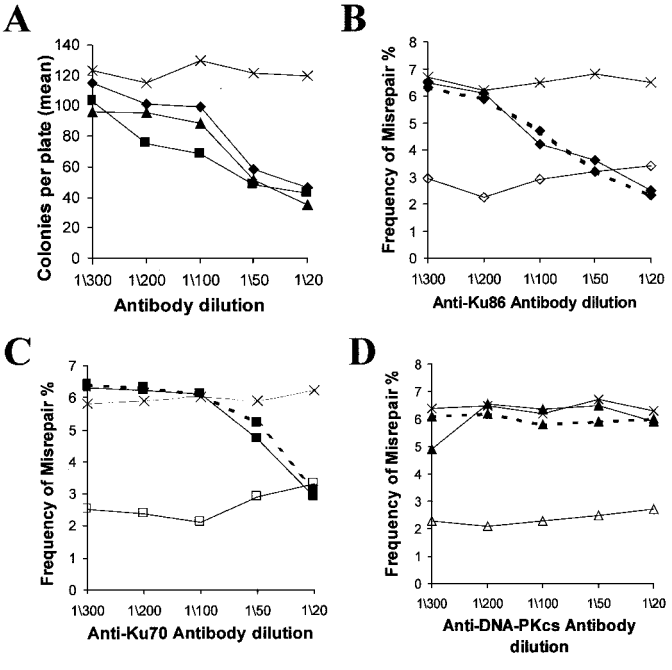

Fig. 5. Frequency of misrepair studies with increasing concentrations of antibodies against NHEJ repair proteins. *A*, graph of the mean number of colonies derived from LacZα reactivation assays after incubation of nuclear extracts with increasing concentration of antibodies to NHEJ proteins. Antibodies are represented by the following symbols: HL60 + anti-Ku86 (◆), HL60 + anti-Ku86 + blocking peptide (*black cross*), HL60 + anti-Ku70 (■), and HL60 + anti-DNA-PKcs (▲). *B*, misrepair frequencies after incubation of nuclear extracts with anti-Ku86: HL60 + anti-Ku86 (◆), HL60 + anti-Ku86 + blocking peptide (*black cross*), AML extract + anti-Ku86 (◆, ····), and normal CD34+ extract + anti-Ku86 (◇). *C*, misrepair frequencies after incubation of nuclear extracts with anti-Ku70: HL60 + anti-Ku70 (■), HL60 + anti-Ku70 + blocking peptide (*black cross*), AML extract + anti-Ku70 (■, ····), and CD34+ extract + anti-Ku70 (□). *D*, misrepair frequencies after incubation of nuclear extracts with anti-DNA-PKcs: HL60 + anti-DNA-PKcs (▲), HL60 + anti-DNA-PKcs + blocking peptide (*black cross*), AML extract + anti-DNA-PKcs (▲, ····), and CD34+ extract + anti-DNA-PKcs (△).

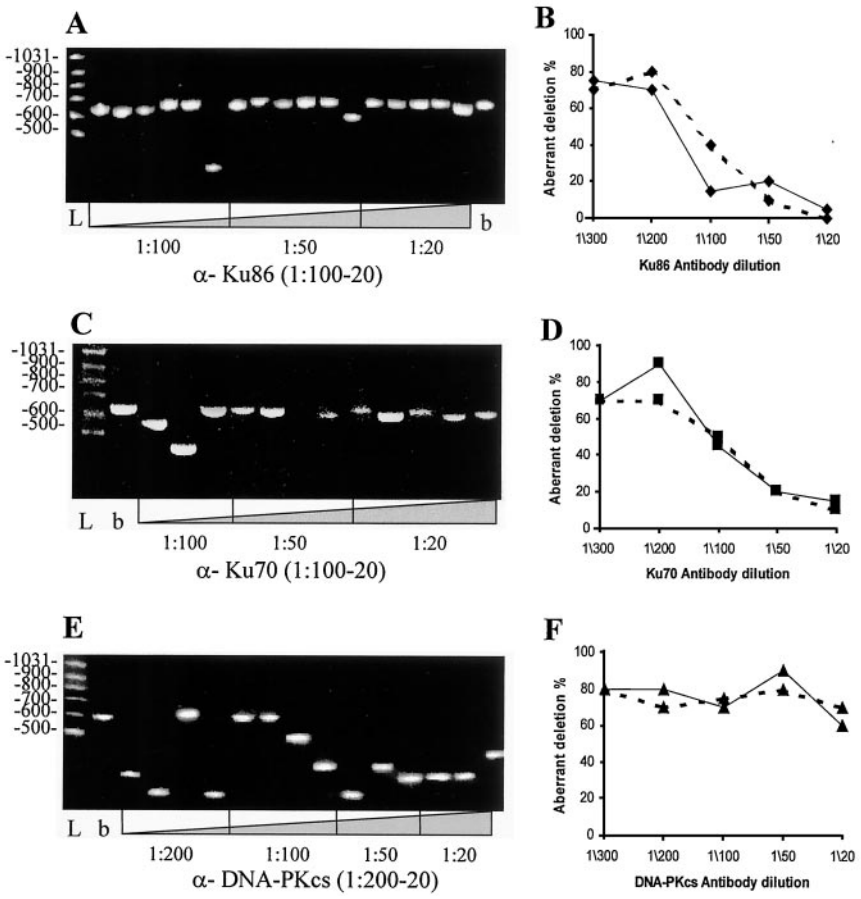

Fig. 6. Repair fidelity studies with increasing concentrations of antibodies against NHEJ repair proteins. *A*, *C*, and *E* PCR products of three to six randomly selected misrepaired colonies from LacZa reactivation experiments using HL60 nuclear extracts incubated with increasing concentrations of antibodies to NHEJ proteins: Anti-Ku86 (*A*; 1:100–1:20) anti-Ku70 (1:100–1:20) and Anti-DNA-PKcs (*B*). *b*, blue colony and *L*, DNA ladder (bp). *B*, *D*, and *F* graphs showing the percentage aberrant deletions with increasing antibody concentration. *B*, experiments using anti-Ku86. HL60 + anti-Ku86 (◆) and AML extract + anti-Ku86 (◆, ····). *D*, experiments using anti-Ku70, HL60 + anti-Ku70 (■), and AML extract + anti-Ku70 (■, ····). *F*, experiments using anti-PKcs, HL60 + anti-DNA-PKcs (▲), and AML extract + anti-DNA-PKcs (▲, ····). White PCR products < 600 bp (>28 bp deletion) were considered aberrant, and thus, the percentage of aberrant deletions was derived by dividing the number of aberrant PCR products by the total number of colonies.

of accompanying DSB repair. The basis for the repair infidelity of the Ku70/86 heterodimer is unclear, because no significant differences in the steady-state expression of key NHEJ proteins were observed to account for this over-activity. However, variant Ku86 has been reported in the HL60 cell line, resulting in altered DNA-binding activity (24). This suggests that other mechanisms, such as mutation of either Ku70 or 86, or post-translational modification of these or other Ku-binding proteins may be responsible for the increased end joining and infidelity we observe in myeloid leukemias. Nevertheless, analysis of some of these plasmid deletions suggests that DSB repair occurred through ligation of distant regions of microhomology. These data are contrary to what is known about microhomology-dependent repair, *i.e.*, that this type of repair is normally associated with the absence of Ku (25, 26). The basis for this difference in microhomology-dependent repair in myeloid leukemia cells is unclear at present. However, it may suggest an aberrant Ku-dependent activity in myeloid leukemias.

The repair infidelity observed is a candidate mechanism for producing the chromosomal abnormalities observed in myeloid leukemias *in vivo*. Over-activity of the NHEJ protein apparatus may result in illegitimate joining and aligning of noncontiguous broken DNA ends, leading to translocations and deletions. However, the specific alterations noted in neoplastic cells are probably the result of selection for those rare changes that give the cell a proliferative advantage. Interestingly, in this regard, regions of microhomology have been found at the breakpoints of chromosomal aberrations in leukemia (27). This is *in vivo* evidence in support of the mechanism we have proposed. In addition, we have recently observed an increased infidelity mediated by a Ku-dependent NHEJ in Bloom's syndrome, a preleukemic syndrome characterized by chromosomal instability. In Bloom's syndrome cells corrected by transfection of the *BLM* gene, NHEJ fidelity is restored (28).

Our findings must be viewed in the context of recent studies of cells from $Ku86^{-/-}$ mice, suggesting the importance of this protein for protecting against genetic instability and tumorigenesis (29). $Ku86^{-/-}$ mice had a marked increase in chromosomal instability manifesting as breakage, translocation, and aneuploidy. These changes were accompanied by a significant incidence of B-cell lymphoma. Furthermore, $Ku86^{-/-}/p53^{-/-}$ mice died of lymphomas before 3 months of age. The comparison of these studies to our present work suggests that the role of Ku86 in cancer is complex and that over or under activity could contribute to DNA repair infidelity in neoplastic cells. Our findings suggest that over-activity of the Ku70/Ku86-mediated repair, in the setting of constitutively increased overall NHEJ activity, may be just as injurious to cells and a more common mechanism in myeloid leukemia, as compared with loss of Ku86 function. This process may be analogous to the situation in *Saccharomyces cerevisiae* described by Tsukamoto *et al.* (30), where illegitimate recombination resulting in DNA deletions was found to be mediated by the end-joining proteins, hdf1, a Ku homologue, and other Ku-binding proteins. This work suggests fertile directions for exploring precisely how the increased NHEJ function arises and the factors determining the specific role of the Ku70/86 protein in causing the attendant infidelity in DNA repair.

ACKNOWLEDGMENTS

We thank Guillermina Nickless for DNA sequencing, Barbara Czepulkowski for cytogenetic analysis, and Drs. Shaun Thomas and Stephen Baylin for helpful suggestions while writing the manuscript.

REFERENCES

1. Cahill, D. P., Lengauer C., Yu, J., Riggins, G. J., Willson, J. K., Markowitz, S. D., Kinzler, K. W., and Vogelstein, B. The mutations of mitotic checkpoint genes in human cells. Nature, *392:* 300–303, 1998.
2. Lengauer, C., Kinzler, K. W., and Vogelstein, B. Genetic instability in cancer. Nature, *396:* 643–649, 1998.
3. Vogelstein, B., Fearon, E. R., Hamilton, S. R., Kern, S. E., Preisinger, A. C., Leppert, M., Nakamura, Y., White R., Smits, A. M. M., and Bos, J. L. N. Genetic events during colorectal tumor development. N. Engl. J. Med., *319:* 525–529, 1988.
4. Khanna, K. K., and Jackson S. P. DNA double strand breaks: signaling, repair and the cancer connection. Nat. Genet., *27:* 247–254, 2001.
5. Schar, P. Spontaneous DNA damage, genomic instability, and cancer–when DNA replication escapes control. Cell, *104:* 329–332, 2001.
6. Richardson, C., and Jasin, M. Frequent chromosomal translocations induced by DNA double strand breaks. Nature, *405:* 697–700, 2000.
7. Chu, G. Double strand break repair. J. Biol. Chem., *272:* 24097–24100, 1997.
8. Zdzienicka, M. Z. Mammalian mutants defective in the response to ionizing radiation-induced DNA damage. Mutat. Res., *336:* 203–213, 1995.
9. Mimori, T., and Hardin, J. A. Mechanism of action between ku protein and DNA. J. Biol. Chem., *261:* 10375–10379, 1986.
10. Falzon, M., Fewell, J. W., and Kuff, E. L. EBP-80, a transcription factor closely resembling the human autoantigen ku, recognizes single- to double-strand transitions in DNA. J. Biol. Chem., *268:* 10546–10552, 1993.
11. Gottlieb, T., and Jackson, S. The DNA-dependent protein kinase: requirement for DNA ends and association with ku antigen. Cell, *72:* 131–142, 1993.
12. Grawunder, U., Wilm, M., Wu, X. T., Kulesza, P., Wilson, T. E., Mann, M., and Lieber, M. R. Activity of DNA ligase IV stimulated by complex formation with XRCC4 protein in mammalian cells. Nature (Lond.), *388:* 492–495, 1997.
13. Roth, D. B., Porter T. N., and Wilson, J. H. Mechanism of non homologous recombination in mammalian cells. Mol. Cell. Biol., *5:* 2599–2607, 1985.
14. Roth, D. B., and Wilson, J. H. Non homologous recombination in mammalian cells: role for the short sequence homologies in the joining reaction. Mol. Cell. Biol., *6:* 4295–4304, 1986.
15. Rowley, J. D. Cytogenetic analysis in leukemia and lymphoma: an introduction. Semin. Hematol., *37:* 315–319, 2000.
16. Fenaux, P., Morel, P., and Lai, J. L. Cytogenetics of myelodysplastic syndromes. Semin. Hematol., *33:* 127–138, 1996.
17. Strick, R., Strissel, P. L., Borgers, S., Smith, S. L., and Rowley, J. D. Dietary bioflavanoids induce cleavage in the *MLL* gene and may contribute to infant leukemia. Proc. Natl. Acad. Sci. USA, *97:* 4790–4795, 2000.
18. Jessberger, R., and Berg, P. Repair of deletions and double-strand gaps by homologous recombination in a mammalian *in vitro* system. Mol. Cell. Biol., *1:* 445–457, 1991.
19. Baumann, P., and West, S. C. DNA end-joining catalyzed by human cell-free extracts. Proc. Natl. Acad. Sci. USA, *95:* 14066–14070, 1998.
20. Bradford, M. M. A rapid and sensitive method for the quantitation of microgram quantities of protein utilising the principle of protein dye binding. Anal. Biochem., *72:* 248–254, 1976.
21. North, P., Ganesh, A., and Thacker, J. The rejoining of double-strand breaks in human DNA by human cell extracts. Nucleic Acids Res., *18:* 6205–6210, 1990.
22. Koeffler, H. P., and Golde, D. W. Human myeloid leukemia cell lines. Blood, *56:* 344–350, 1980.
23. Nagai, M., Seki, S., Kitahara, T., Abe, T., Minato, K., Watanabe, S., and Shimoyama, M. A novel human myelomonocytoid cell line. P39/Tsugane, derived from overt leukemia following myelodysplastic syndrome. Gann, *75:* 1100–1107, 1984.
24. Han, Z., Johnson, C., Reeves, W. H., Carter, T., Wyche, J. H., and Hendrickson, E. A. Characterization of a Ku86 variant protein that results in altered DNA binding and diminished DNA-dependent protein kinase activity. J. Biol. Chem., *271:* 14098–14104, 1996.
25. Boulton, S. J., and Jackson, S. P. Saccharomyces cerevisiae Ku70 potentiates illegitimate DNA double-strand break repair and serves as a barrier to error-prone DNA repair pathways. EMBO J., *15:* 5093–5103, 1996.
26. Kabotyanski, E. B., Gomelsky, L., Han, J. O., Stamato, T. D., and Roth, D. B. Double-strand break repair in Ku86- and XRCC4-deficient cells. Nucleic Acids Res., *26:* 5333–5342, 1998.
27. Weimels, J. L., and Greaves, M. Structure and possible mechanism of TEL-AML1 gene fusions in childhood acute lymphoblastic leukemia. Cancer Res., *59:* 4075–4082, 1999.
28. Gaymes, T. J., North, P. S., Brady, N., Hickson, I. D., Mufti, G. J., and Rassool, F. V. Increased error-prone non homologous end-joining–A proposed mechanism of chromosomal instability in Bloom's Syndrome. Oncogene, *21:* 2525–2533, 2002.
29. Difilipiantonio, M. J., Zhu, J., Chen, H. T., Meffre, E., Nussenzweig, M. C., Max, E. E., Ried, T., and Nussenzweig, A. DNA repair protein ku80 suppresses chromosomal aberrations and malignant transformation. Nature, *400:* 510–513, 2000.
30. Tsukamoto, Y., Kato, J., and Ikeda, H. Silencing factors participate in DNA repair and recombination in. Saccharomyces cerevisiae. Nature, *388:* 900–903, 1997.

Myeloid Leukemias Have Increased Activity of the Nonhomologous End-Joining Pathway and Concomitant DNA Misrepair that Is Dependent on the Ku70/86 Heterodimer

Terry J. Gaymes, Ghulam J. Mufti and Feyruz V. Rassool

Cancer Res 2002;62:2791-2797.